

# Bridging 3D Gaussian and Mesh for Freeview Video Rendering

YUTING XIAO, ShanghaiTech University, China and Ant Group, China

XUAN WANG, Ant Group, China

JIAFEI LI, Xi'an Jiaotong University, China and Ant Group, China

HONGRUI CAI, University of Science and Technology of China, China and Ant Group, China

YANBO FAN, Ant Group, China

NAN XUE, Ant Group, China

MINGHUI YANG, Ant Group, China

YUJUN SHEN, Ant Group, China

SHENGHUA GAO, ShanghaiTech University, China

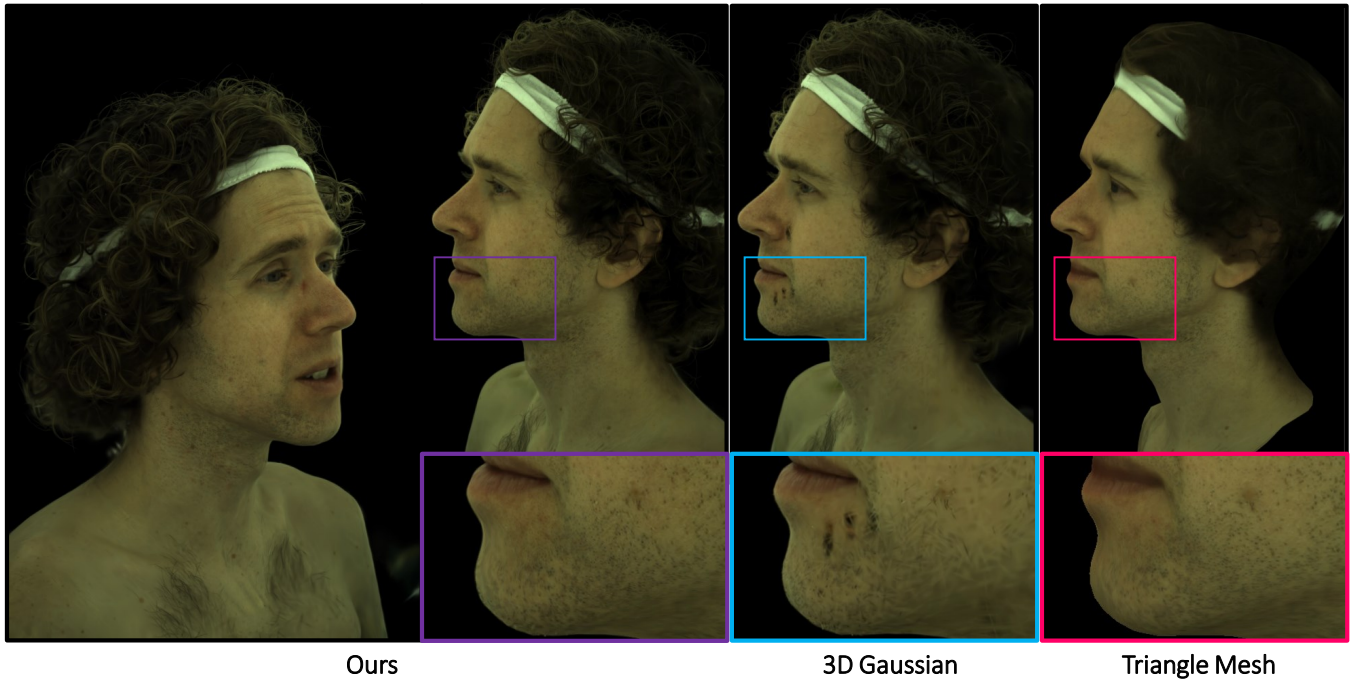


Fig. 1. We are introducing a new technology called **GauMesh** that combines the benefits of 3D Gaussian and triangle mesh primitives to create a more effective view synthesis of dynamic scenes. Our method can capture complex microstructures of geometry and sharp, detailed textures without leaving any holes, as depicted in the figure.

Authors' addresses: Yuting Xiao, ShanghaiTech University, China and Ant Group, China; Xuan Wang, Ant Group, China; Jiafei Li, Xi'an Jiaotong University, China and Ant Group, China; Hongrui Cai, University of Science and Technology of China, China and Ant Group, China; Yanbo Fan, Ant Group, China; Nan Xue, Ant Group, China; Minghui Yang, Ant Group, China; Yujun Shen, Ant Group, China; Shenghua Gao, ShanghaiTech University, China;

Permission to make digital or hard copies of all or part of this work for personal or classroom use is granted without fee provided that copies are not made or distributed for profit or commercial advantage and that copies bear this notice and the full citation on the first page. Copyrights for components of this work owned by others than ACM must be honored. Abstracting with credit is permitted. To copy otherwise, or republish, to post on servers or to redistribute to lists, requires prior specific permission and/or a fee. Request permissions from [permissions@acm.org](mailto:permissions@acm.org).

© 2024 Association for Computing Machinery.

0730-0301/2024/3-ART \$15.00

<https://doi.org/10.1145/nnnnnnn.nnnnnnn>

Recently, primitive-based rendering has been proven to achieve convincing results in solving the problem of modeling and rendering the 3D dynamic scene from 2D images. Despite this, in the context of novel view synthesis, each type of primitive has its inherent defects in terms of representation ability. It is difficult to exploit the mesh to depict the fuzzy geometry. Meanwhile, the point-based splatting (e.g. the 3D Gaussian Splatting) method usually produces artifacts or blurry pixels in the area with smooth geometry and sharp textures. As a result, it is difficult, even not impossible, to represent the complex and dynamic scene with a single type of primitive. To this end, we propose a novel approach, **GauMesh**, to bridge the 3D **Gaussian** and **Mesh** for modeling and rendering the dynamic scenes. Given a sequence of tracked mesh as initialization, our goal is to simultaneously optimize the mesh geometry, color texture, opacity maps, a set of 3D Gaussians and the deformation field. At a specific time, we perform  $\alpha$ -blending on the RGB and opacity values based on the merged and re-ordered z-buffers from mesh

and 3D Gaussian rasterizations. This produces the final rendering, which is supervised by the ground-truth image. Experiments demonstrate that our approach adapts the appropriate type of primitives to represent the different parts of the dynamic scene and outperforms all the baseline methods in both quantitative and qualitative comparisons without losing render speed.

CCS Concepts: • **Do Not Use This Code** → **Generate the Correct Terms for Your Paper**; *Generate the Correct Terms for Your Paper*; Generate the Correct Terms for Your Paper; Generate the Correct Terms for Your Paper.

Additional Key Words and Phrases: Freeview Video, Primitive-based Rendering, Novel view synthesis, 3D Gaussian splatting

#### ACM Reference Format:

Yuting Xiao, Xuan Wang, Jiafei Li, Hongrui Cai, Yanbo Fan, Nan Xue, Minghui Yang, Yujun Shen, and Shenghua Gao. 2024. Bridging 3D Gaussian and Mesh for Freeview Video Rendering. *ACM Trans. Graph.* 1, 1 (March 2024), 9 pages. <https://doi.org/10.1145/nnnnnnn.nnnnnnn>

## 1 INTRODUCTION

Neural radiance field (NeRF) rendering techniques [Mildenhall et al. 2020] have achieved a significant advancement in the field of novel view synthesis and have been quickly incorporated into the process of modeling and rendering dynamic scenes. Vanilla NeRF techniques use the implicit neural representation to depict the 3D scene, which requires extensive queries of a Multi-Layer Perceptron (MLP) resulting in inefficient training and rendering. The 3D Gaussian Splatting (3DGS) [Kerbl et al. 2023] has been proposed to solve the limitations, which is a primitive-based method that represents the 3D scene as a set of explicit 3D Gaussian ellipsoids. Many concurrent works introduce the 3DGS into the construction of free-view video of a dynamic scene.

Exploiting primitive-based rendering in free-view video modeling far predates the dynamic 3DGS. In the early stage, the tracked mesh (usually the triangle mesh) is employed as the 3D representation to depict the dynamic scene. There are two main problems with the mesh generated by Multi-View Stereo (MVS). Firstly, it can be noisy and incomplete. Secondly, it is not able to accurately represent microstructures. While 3DGS exploits the multiple overlapped 3D Gaussian ellipsoids to represent the fuzzy geometry well, it solves these issues and produces a more accurate output. However, the 3DGS method couples geometry and texture representations, requiring a large number of 3D points to capture complex microstructures and detailed textures on smooth surfaces. As a consequence, it will produce more artifacts or blurry pixels in the area with smooth geometry and sharp texture details than using a mesh with a texture map. In summary, it is quite difficult to represent the 3D scene well with a single primitive type.

In this paper, we present a novel framework (GauMesh) that employs the hybrid primitive types, i.e. triangle mesh and 3D Gaussians, within a differentiable rendering pipeline. The framework is strategically designed to leverage the strengths of each primitive type: high-resolution textured triangle meshes excel at modeling complex and detailed color appearances on smooth surfaces, whereas 3D Gaussians can do well in complex geometries. We design a hybrid rendering pipeline that can adaptively fuse these two primitive types, leading to better rendering performance than only applying a single representation. To be specific, for each pixel under a specific view, we first apply the mesh rasterization technique to

get its values of depth, opacity, and color. Then, the rasterization w.r.t. the pixel in the 3D Gaussian Splatting [Kerbl et al. 2023] yields a list of points, each with one depth value. We treat the result of mesh rasterization as one point and intersect it into the point list of Gaussians according to the order of depth. After the intersection, the  $\alpha$ -blending is exploited to compute the pixel colors.

Then, we adopt the rendering of hybrid primitives in the 4D optimization scheme. Given the multi-view videos of a dynamic scene, we first apply a mesh to point cloud registration algorithm to track the mesh from one keyframe to the next with a fixed texture map. Then we initialize the 3D Gaussians according to the tracked meshes and utilize a grid-based feature volume to model the deformation field of the 3D Gaussians. We adopt a joint optimization process that refines both the appearance of the mesh and the deformed 3D Gaussians across temporal and spatial dimensions.

The experimental results demonstrate that the method presented in this study outperforms previous approaches and obtains superior visual quality. Our GauMesh is capable of adaptively representing a 3D dynamic scene using appropriate primitive types. It can model fuzzy geometry and sharp, detailed textures with high quality simultaneously.

## 2 RELATED WORK

In this section, we provide a concise review of various representations for view synthesis in dynamic scenes. We delve into these representations, spanning from implicit neural representation to explicit geometries, and highlight their respective strengths and limitations. Furthermore, we draw attention to hybrid representations, elucidating the relationship between our method and previous approaches.

*Implicit Neural Representation (INR)*. There are various methods that use the INR as a Signed Distance Function (SDF) [Chabra et al. 2020; Jiang et al. 2020; Park et al. 2019] or occupancy field [Genova et al. 2020; Mescheder et al. 2019; Peng et al. 2020; Saito et al. 2019, 2020]. These methods are implemented by MLPs and are used to represent the geometry of a static or even dynamic 3D scene [Niemeyer et al. 2019]. NeRF [Mildenhall et al. 2020] is proposed to model the 3D scene as a neural radiance field with the INR which has made great progress in the task of view synthesis. Due to its powerful appearance modeling ability, NeRF techniques have been rapidly introduced to the dynamic domain. Techniques like Nerfies [Park et al. 2021a], D-NeRF [Pumarola et al. 2021] and etc. [Du et al. 2021] take time indices as additional inputs of the MLP to model the dynamics. Then the hyperspace [Park et al. 2021b] and is exploited a priori to improve the modeling capacity in visual quality. By cooperating with human priors, NeRF techniques can also model the animatable avatars [Peng et al. 2021a; Su et al. 2021]. However, all the above methods suffer from the same defects. One is that they require massive MLP queries which makes the rendering inefficient. The other is that the implicit geometry is difficult to control, especially in the case of dynamic modeling and animation.

*Voxel-based Representation*. Many 3D rendering approaches rely on a uniform dense voxel grid to represent the geometry or appearance of an object. DeepVoxels [Sitzmann et al. 2019] stores a feature grid and uses a learned U-Net to render the projected feature map.

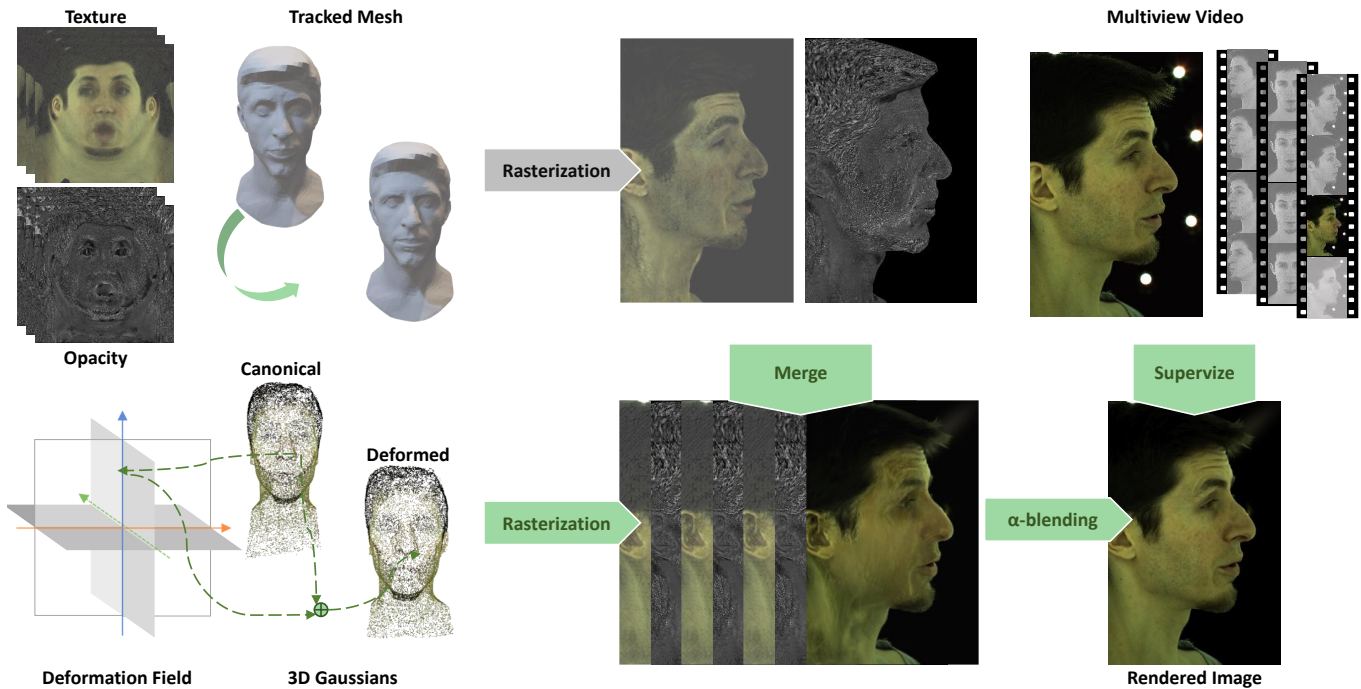


Fig. 2. The overall pipeline of GauMesh. Given the calibrated multiview videos and the corresponding tracked mesh, in addition to the 3D Gaussian’s properties, the presented method learns the mesh sequence, time-varying opacity, and texture maps from the image observation via hybrid differentiable rendering.

Plenoxols [Fridovich-Keil et al. 2022] encodes the radiance field in an explicit and sparse voxel with spherical harmonics, which increases render speed but still requires a dense initial grid for optimization. NeuralVolumes [Lombardi et al. 2019] uses a voxel-based representation in dynamic cases and a warping field to encode a sparse target volume into a denser template volume. Despite their benefits, voxel-based methods can suffer from the cubic storage complexity of dense voxel grids and lead to over-smoothed pixels.

*Geometric Primitive Representation.* The two main geometric primitive representation are triangle meshes and 3D points. Mesh-based representation is popular in computer graphics and is used to model Freeview videos [Collet et al. 2015] at an early stage. When a perfect mesh is available, it can be used to create photorealistic images of high quality. In recent years, differentiable rendering techniques [Munkberg et al. 2022] have been used to recover mesh and textures from 2D images using various tools like PyTorch3D [Ravi et al. 2020], Nvidia’s DiffRast [Laine et al. 2020] and etc. [Kato et al. 2018; Loper and Black 2014; Valentin et al. 2019; ?] However, generating accurate mesh is still difficult and often results in incomplete or noisy reconstructions. 3D points are the simplest geometric primitive used for both geometry and appearance modeling, but suffer from temporal instability and holes. A promising approach, 3DGS [Kerbl et al. 2023], has been proposed to represent 3D scenes using multiple overlapped Gaussian ellipsoids. This method is optimized using differentiable rendering and is good at modeling fuzzy geometry with extremely fast rendering and can also be used to

model dynamic scenes [Luiten et al. 2023]. However, it requires a large number of 3D points to capture both geometric and appearance details, leading to artifacts on smooth surfaces, especially when the texture is sharp and detailed.

*The Hybrid Modeling.* Many techniques attempt to improve the render quality by using hybrid modeling with multiple representations. In the case of NeRF, some methods use feature voxels [Liu et al. 2020; Sun et al. 2022] to encode the 3D scene, requiring only a small MLP to decode the sampled features into color and density. A human prior can also be used, making it convenient for performance capture [Chen et al. 2023b; Peng et al. 2021b]. Then the tri-plane [Chan et al. 2022], tensor decomposition [Chen et al. 2022], sparse feature voxel and the hash grid [Müller et al. 2022] are exploited to replace the dense voxels, which can be extended to the dynamic case [Fang et al. 2022; Song et al. 2023; Wang et al. 2023; ?; ?]. Other works use pre-sampled strategies to bake the neural radiance into explicit representations, such as mesh [Chen et al. 2023a], sparse voxels [Yu et al. 2021] and etc [Hedman et al. 2021]. However, these hybrid methods still inherit the defects of MLP-based techniques. Mixtures of Primitives (MVP) presents a more efficient hybrid approach, which represents the dynamic 3D scene with multiple voxel grids anchored to a tracked mesh. It uses explicit representation, and the voxel grids are sparse in the entire 3D space since they are anchored on a surface. MVP produces comparable or better quality compared to voxel-based and implicit neural representation-based methods and supports relatively efficient rendering. For 3DGS, it

can also be extended to dynamic scenes by exploiting an additional deformation field with a hybrid representation [Wu et al. 2023].

*Summary.* We introduce the concept of a hybrid representation, which combines geometric primitives that are hardware-friendly for rendering. This representation merges the triangle mesh and point-based 3D Gaussians into a single rendering pipeline that is differentiable. By using our differentiable hybrid rendering in conjunction with a tracked mesh, we can create a dynamic scene that adapts to the proper primitives and captures the complex microstructure of geometry and sharp texture details simultaneously.

### 3 METHOD

Given a multiview video recording of the dynamic 3D scene, the objective of freeview video rendering is to reconstruct the underlying 3D environment and generate real-time novel views from any perspective. Our approach uniquely combines 2 explicit representations: the 3D Gaussian [Kerbl et al. 2023] and Polygon Mesh for hybrid rendering. By leveraging alpha-composition techniques, we effectively merge these two representations to create a hybrid rendering method. Our method can fuse the advantages from both representations and achieve detailed reconstruction for the sharp feature and complex geometry.

The pipeline of our method is shown in Figure. 2. Firstly, we introduce the hybrid rendering approach of 3D Gaussians and triangle mesh. We blend these two representations to render scenes with high fidelity and detail. Second, we apply the grid-based representation for modeling the deformation field of 3D Gaussians and tracking the reconstructed mesh from the keyframe to other frames which allows us to track the changes in the scene from keyframe to other frames accurately. Third, we introduce the optimization for the proposed hybrid representation for dynamic scene reconstruction.

#### 3.1 Preliminary

We simply review the rendering pipeline of 3D Gaussian representation in this section. 3D Gaussian is a point-based explicit representation that models the object as the combination of multiple Gaussian kernels. Each 3D Gaussian has a covariance matrix  $\Sigma$  and a 3D coordinate to represent the center of the 3D Gaussian. These 2 elements are the geometry information of 3D Gaussians:

$$G(x) = e^{-\frac{1}{2}(x)^T \Sigma^{-1}(x)} \quad (1)$$

The 3D Gaussian is projected to 2D image space for the  $\alpha$  blending process. The projection formulation is defined as:

$$\Sigma' = JW\Sigma W^T J^T \quad (2)$$

where the  $W$  and  $\Sigma'$  are the viewing transformation matrix and covariance matrix in the camera coordinate. The affine approximation of the projective is the Jacobian  $J$ .

The  $\Sigma$  can be computed by the scaling matrix  $s$  and rotation matrix  $r$ :

$$\Sigma = RSS^T R^T \quad (3)$$

Each 3D Gaussian is characterized by several elements: position  $\mathcal{X}$ , the color feature defined by the spherical harmonic (SH)  $C$ , opacity  $\alpha$ , rotation represented by the quaternion  $r$ , and scaling factor  $s$ . The rendered color of a specific pixel can be computed by the volumetric rendering technique.

#### 3.2 Hybrid Rendering

Our target is to represent a dynamic scene with 3D Gaussians [Kerbl et al. 2023] and polygon mesh. The 3D Gaussian is more suitable for constructing complex geometric structures while the mesh is more suitable for reconstructing the detailed color appearance on the smooth surface. Both of them are explicit representations so real-time rendering is still allowed.

Our methodology presents a novel, integrated approach that combines two explicit representations to exploit their inherent advantages while circumventing their limitations. The core principle of this method revolves around the combination of 3D Gaussian and triangle mesh.

We utilize Nvdiffrast [Laine et al. 2020] which applies the Anti-alias method on mesh rasterization to achieve differentiable rendering for the mesh. Given a mesh, an alpha UV map and an SH(spherical harmonics) UV map are defined to describe the transmittance and color appearance of each face, we rasterize the mesh from a specific viewpoint to obtain the depth map  $D'$ , the opacity map  $A'$ , and color map  $C'$ . Suppose the depth, alpha value, and color of a pixel  $\mathbf{u}$  on each map are  $d'$ ,  $\alpha'$ , and  $\mathbf{c}'$  respectively. The 3D Gaussians are projected on the 2D image plane for rendering, denote the depth, opacity, and color on the  $i^{th}$  point on the ray corresponding to the specific pixel  $\mathbf{u}$  as  $d_i$ ,  $\alpha_i$  and  $\mathbf{c}_i$ . The depth of a 3D Gaussian is defined as the distance towards the center of the Gaussian, which follows the 3DGS [Kerbl et al. 2023]. If  $d_i < d' < d_{i+1}$ , computing the color of pixel  $\mathbf{u}$  by blending process as :

$$C(\mathbf{u}) = T' \alpha' \mathbf{c}' + \sum_{k=1}^K T_k \alpha_k \mathbf{c}_k \quad (4)$$

where the  $T'$  and  $T_k$  are defined as:

$$T' = \prod_{j=1}^i (1 - \alpha_j), \quad T_k = \mathbb{1}(d', d_k, \alpha') \prod_{j=1}^{k-1} (1 - \alpha_j) \quad (5)$$

The  $\mathbb{1}(d', d_k, \alpha')$  is an identity function for intersecting the point on the mesh to the point list of 3D Gaussians:

$$\mathbb{1}(d', d_k, \alpha') = \begin{cases} 1 & , if \quad d' > d_k \\ \alpha' & , if \quad d' \leq d_k \end{cases} \quad (6)$$

The illumination of the hybrid rendering is shown in Figure. 2

#### 3.3 Hybrid Deformation Field

Given the 3D coordinates of a Gaussian, we represent its position, scale, rotation, and opacity in the temporal space by utilizing the deep neural network and tri-plane feature grid [Cao and Johnson 2023; Chen et al. 2022; Fridovich-Keil et al. 2023]. Specifically, following the 4DGaussian [Wu et al. 2023], given a 3D Gaussian in the canonical space, we apply a multi-resolution Hexplane [Cao and Johnson 2023] and shallow MLP  $\phi$  to extract and decode the features from a 4D K-Planes module [Fridovich-Keil et al. 2023] which contains 6 feature planes according to the position in canonical space  $\mathbf{x}_c = (x, y, z)$  and time  $t$ . We can decode the position, scale, rotation, and opacity of the 3D Gaussian at any given point in the temporal sequence, thereby enabling a robust and detailed representation of the dynamic scene deformation field modeling.

Specifically, the extracted features on the spatial and temporal space are denoted as

$$\mathcal{D}(x, y, z, t) = \{D_l(x, y), D_l(y, z), D_l(x, z), D_l(x, t), D_l(y, t), D_l(z, t) | l \in \{1, 2\}\} \quad (7)$$

where the  $l$  is the upsampling scale and the  $D_l(i, j)$  is the multi-resolution feature plane.

After the features  $D_l(i, j)$  from multiple feature planes are obtained, they are fused to a global feature vector which consists of both temporal and spatial information:

$$\mathcal{H} = \bigcup_i \prod \text{interp}(D_l(y, z), D_l(x, z), D_l(x, t), D_l(y, t), D_l(z, t)) \quad (8)$$

where the "interp" indicates the bilinear interpolation for the 2D feature grid plane. Take the position parameter  $\mathbf{x}$  of 3D Gaussian as an example, the deformed position can be computed by decoding the feature vector:  $\mathbf{x}(t) = \mathbf{x}_c + \phi_{\mathbf{x}}(\mathcal{H})$ . The  $\phi_{\mathbf{x}}$  is the shallow MLP for decoding the position deformation of 3D Gaussian. This design is also applied to the scale, rotation, and opacity parameters of 3D Gaussians.

For the mesh representation, since the deformation of mesh has a different pattern from the 3D Gaussian, we design the deformation of mesh as the translation of each vertex instead of applying a grid-based field, which is a simpler and more direct approach. In this case, each vertex in the mesh has its own displacement vector, which directly translates it from its original position to a new position in the deformed state. The mesh-based representation contains the mesh, opacity map, and texture feature map for each frame with a shared topological structure.

### 3.4 Optimization Strategy

In the initial phase of our method, we tackle the challenge of tracking a mesh representation in a dynamic scene using a keyframe-based approach. Specifically, we utilize Reality Capture Software to generate a high-quality textured mesh for a selected keyframe. This keyframe mesh serves as the base model against which other frames are registered and aligned. Next, we apply the mesh to the point cloud registration algorithm AMM-NRR [Yao et al. 2023] to establish the mesh-to-points correspondences and get coarse-tracked meshes to other frames.

Subsequently, we refine the tracked meshes further using the differentiable rendering framework Nvdiffrast [Laine et al. 2020] to refine the tracked mesh of each frame by applying the photometric loss  $\mathcal{L}_2$  ensuring that the rendered image closely matches the actual input images from each frame. And the normal consistency loss  $\mathcal{L}_{nc}$  to ensure that the surface normals across the mesh faces align well with those estimated from the input data. During this refinement process, the opacity UV map for all the tracked meshes is set to 1 which indicates full visibility, and the opacity and texture map are not subject to optimization, focusing solely on refining the geometry according to the photometric and normal constraints from the dynamic scene.

The photometric loss for the mesh tracking is defined as the  $L_2$  norm term:

$$\mathcal{L}_2 = \sum_{\mathbf{u} \in \mathcal{U}} \|\mathbf{C}(\mathbf{u}) - \mathbf{C}_{gt}(\mathbf{u})\|_2^2 \quad (9)$$

where the  $\mathcal{U}$  is the set of the pixels on the image. The loss function corresponding to this non-rigid tracking phase is:

$$\mathcal{L}_m = \mathcal{L}_2 + \lambda_{nc} \mathcal{L}_{nc} \quad (10)$$

where the  $\mathcal{L}_{nc}$  is the normal consistency loss for smooth regularization to the mesh.

After the non-rigid tracking of meshes, we initialize the point cloud of 3D Gaussians in canonical space according to the tracked mesh of each frame. For the linear layer  $y = Wx + b$  of MLP for decoding the deformation feature vector, the learnable parameters  $W$  are initialized as normal distribution  $\mathcal{N}(0, \epsilon)$ , where the  $\epsilon$  is a small value (1e-4), and the learnable parameters  $b$  are initialized as zero. This deformation field initialization can guarantee the deformations are close to zero at the beginning of the training phase, such that there are initialized 3D Gaussians close to the surface for every frame. The vertices, opacity map, and texture feature map from mesh representation are all optimized in this phase.

The loss function of optimizing the hybrid representation is:

$$\mathcal{L} = \lambda_1 \mathcal{L}_1 + \lambda_{SSIM} \mathcal{L}_{SSIM} + \lambda_{tv} \mathcal{L}_{tv} \quad (11)$$

where  $\mathcal{L}_1$  and  $\mathcal{L}_{SSIM}$  is the  $L_1$  norm loss and structural similarity loss between the rendered image and ground truth image. The  $\mathcal{L}_{tv}$  is the Total Variational (TV) loss on the feature plane of the deformation field on the spatial and temporal range, which follows the Hexplane [Cao and Johnson 2023]. This loss function is applied to the feature plane of the deformation field across both spatial and temporal dimensions to ensure the smoothness of the deformation field.

## 4 IMPLEMENTATION DETAILS

In our approach to dynamic scene reconstruction, we leverage the Reality Capture Software for the initial 3D mesh reconstruction at each keyframe and for generating point clouds from the other frames. To align these meshes with their corresponding point clouds, we utilize the AMM-NRR method AMM-NRR [Yao et al. 2023] for the keyframe mesh to point cloud registration from other frames. We optimize the vertices in 10 iterations with  $\lambda_{nc} = 0.005$  and normal consistency loss for mesh. After non-rigid mesh tracking, we initialize 100000 points and train 80000 iterations for dynamic scene reconstruction with hybrid representation. The  $\lambda_1 = 0.4$ ,  $\lambda_{SSIM} = 0.6$ ,  $\lambda_{tv} = 0.001$ . The temporal resolution of the feature plane is set the half of the number of frames. Our method takes about 2 minutes to track the mesh from the keyframe to another single frame. The training time for 80000 iterations would take about 5 hours on a single NVIDIA RTX A6000 GPU.

## 5 EXPERIMENTS

**Datasets.** We train and evaluate our method **GauMesh** on the high-quality multi-view dynamic scene datasets: Multiface [Wuu et al. 2022]. The Multiface dataset is a challenging benchmark that contains intricate facial geometries and fine-grained color details,



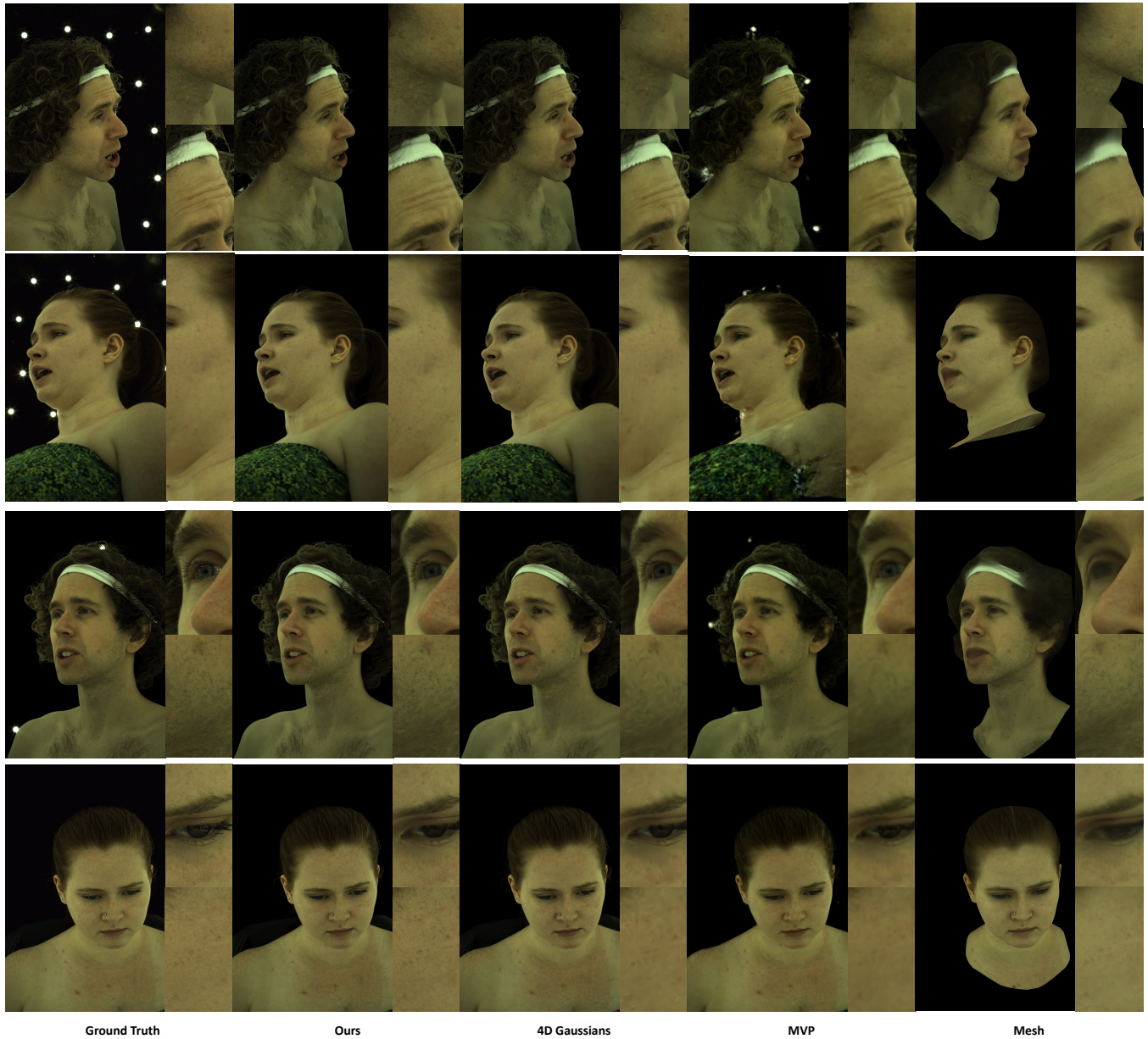


Fig. 3. The qualitative experiments on the test views of the Multiface dataset [Wuu et al. 2022], our method can reconstruct the complex geometry structure and detailed color appearance on the smooth surface better than other baselines. Zoom in for a better view.

which demand high-fidelity reconstruction techniques. The Multiface dataset consists of high-quality recordings of human faces. We select 4 identities with 2K cameras at 30 FPS. 2 identities have about 150 cameras and the other 2 identities have about 40 cameras. Since the Multiface dataset provides the tracked mesh of each frame, we utilize the tracked mesh in the official data. For Both datasets, We choose 90% views as the training set and the rest views as the test set.

**Baselines.** To validate the robustness and effectiveness of our proposed model in dynamic reconstruction tasks, we have carried out comparative experiments against a series of state-of-the-art methods: (i) Explicit representation for dynamic reconstruction: MVP [Lombardi et al. 2021]; (ii) Combination of implicit neural network and explicit representation: 4DGaussians [Wu et al. 2023].

**Metrics.** We utilize 3 different metrics for evaluation. (I) The Peak Signal-to-Noise Ratio (PSNR), is a classical metric in image and signal processing that measures the ratio between the maximum

Method	Ours	4DGaussians	MVP	Mesh
PSNR	<b>34.23</b>	33.76	32.98	21.562
SSIM	<b>0.8872</b>	0.8789	0.8648	0.6747
LPIPS	<b>0.1320</b>	0.1636	0.1612	0.2759

Table 1. The quantitative comparison experiments on the Multiface dataset. Our method achieves state-of-the-art performance than other methods. Since our model can reconstruct the details on the smooth surface better than only applying 3D Gaussians, the improvements are more obvious on LPIPS metrics

possible power of a signal and the power of corrupting noise that affects the fidelity of its representation. (ii) Structural Similarity Index (SSIM) serves as another key criterion for our evaluation. SSIM takes into account not only the luminance and contrast but also the structural information present within the images. (iii) The Learned Perceptual Image Patch Similarity (LPIPS) measure, which represents a more recent advancement in evaluating visual quality. LPIPS computes perceptual differences between images by feeding them into a deep neural network trained on large-scale datasets for image classification tasks.

### 5.1 Comparative Experiments

The qualitative and quantitative results on the Multiface dataset [Wuu et al. 2022] are shown in Fig. 3 and Table. 1. It can be observed that our method achieves state-of-the-art performance compared with other baselines which indicates its superior performance over existing baselines. This highlights the robustness and effectiveness of our proposed hybrid representation for freeview video rendering.

The 4DGaussian [Wu et al. 2023] modeling the deformation of canonical 3D Gaussians [Kerbl et al. 2023] can effectively reconstruct intricate geometries like hair strands with high fidelity. However, despite its strengths in handling complex structures, this method tends to lose subtle details when it comes to smooth surfaces, such as the fine whiskers on a human face.

Meshes are inherently well-suited for representing smooth surfaces because they allow for modeling the surface over vertices and topology, thereby enabling the capture of minute surface variations.

Our method can not only preserve the high-fidelity reconstruction of the hair but also reconstruct the detailed color appearance of the human face. This indicates that our method has a significantly better capacity for the details on the smooth surface, which benefits from the mesh representation. The mesh is suitable for representing the smooth surface and the high-resolution texture feature map can achieve the representing for complex color appearance and only occupy very little memory.

### 5.2 Visualization of Hybrid Representation

Our innovative approach integrates two explicit representation techniques to maximize their complementary strengths and mitigate their respective weaknesses. By employing 3D Gaussians, we can effectively tackle complex geometric structures, capturing volumetric information with high precision and flexibility. Textured meshes excel in representing surface details and color appearances on simpler, more well-defined surfaces. As a result, this hybrid rendering

technique delivers a comprehensive and visually compelling performance.

As demonstrated in Fig. 4, we visualize the rendering results of hybrid representation, only rendering 3D Gaussians, and only rendering mesh. This visualization effectively elucidates the distinct roles and contributions of each component in the reconstruction process. We can observe that the results rendered by employing only 3D Gaussians showcase an approximation of the overall geometric form of the target object. The 3D Gaussian representation is adept at capturing the complex geometry structure and general shape characteristics but may lack the fine-grained color details that are typically found on smooth surfaces. While the textured mesh mainly holds the details on the smooth surface, such as the scum, freckles, and small wrinkles on the face, which results in a comprehensive and visually compelling recreation of the target object.

This visual ablation study thus substantiates the effectiveness and necessity of our proposed hybrid representation strategy in achieving superior rendering performance.

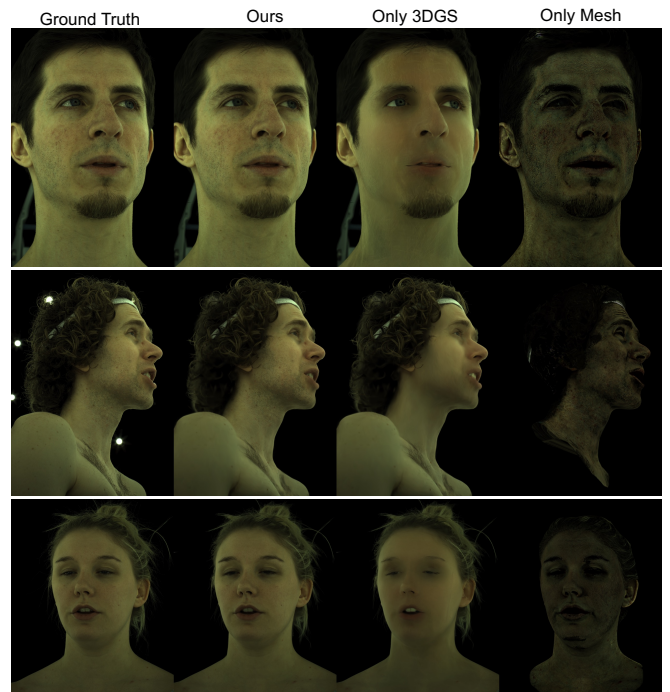


Fig. 4. Our render pipeline combines the 3D Gaussian splitting and mesh representation for hybrid rendering. We demonstrate the rendering results for each component. It can be observed that the 3D Gaussians mainly represent the geometry well but lack the details in color appearance, while the mesh representation mainly focuses on the detailed features on the smooth surface.

## 6 CONCLUSION

In this paper, we present a novel hybrid representation called GauMesh that integrates the strengths of two distinct explicit 3D representations: the 3D Gaussian Splatting [Kerbl et al. 2023] and traditional

mesh-based models. This approach aims to optimize freeview video rendering by leveraging the best features from both methods. A deformation field applying the vector quantization for compression is utilized for modeling the deformation from canonical 3D Gaussian space to the time-varying space. To deform the mesh on time-space, we apply the mesh to the point cloud registration method AMM-NRR and differentiable rendering toolbox Nvdiffrast [Laine et al. 2020] for tracking the mesh. Such that we can obtain the hybrid representation along the time-space. The hybrid representation can exert advantages over each other. The 3D Gaussian is suitable for modeling complex and detailed geometry while the triangle mesh representation can reconstruct the fine color appearance by the high-resolution texturing. Our **GauMesh** model can also preserve the advantages of fast rendering since the 3D Gaussian and mesh can both be rendered by rasterization, which indicates high-quality rendering in real-time.

## REFERENCES

- Ang Cao and Justin Johnson. 2023. Hexplane: A fast representation for dynamic scenes. In *Proceedings of the IEEE Conference on Computer Vision and Pattern Recognition*. 130–141.
- Rohan Chabra, Jan Eric Lenssen, Eddy Ilg, Tanner Schmidt, Julian Straub, Steven Lovegrove, and Richard Newcombe. 2020. Deep Local Shapes: Learning Local SDF Priors for Detailed 3D Reconstruction. In *Proceedings of the European Conference on Computer Vision*. Springer, 608–625.
- Eric R Chan, Connor Z Lin, Matthew A Chan, Koki Nagano, Boxiao Pan, Shalini De Mello, Orazio Gallo, Leonidas J Guibas, Jonathan Tremblay, Sameh Khamis, et al. 2022. Efficient geometry-aware 3D generative adversarial networks. In *Proceedings of the IEEE Conference on Computer Vision and Pattern Recognition*. 16123–16133.
- Anpei Chen, Zexiang Xu, Andreas Geiger, Jingyi Yu, and Hao Su. 2022. Tensor3D: Tensorial radiance fields. In *Proceedings of the European Conference on Computer Vision*. Springer, 333–350.
- Yue Chen, Xuan Wang, Xingyu Chen, Qi Zhang, Xiaoyu Li, Yu Guo, Jue Wang, and Fei Wang. 2023b. UV Volumes for real-time rendering of editable free-view human performance. In *Proceedings of the IEEE Conference on Computer Vision and Pattern Recognition*. 16621–16631.
- Zhiqin Chen, Thomas Funkhouser, Peter Hedman, and Andrea Tagliasacchi. 2023a. Mobilenerf: Exploiting the polygon rasterization pipeline for efficient neural field rendering on mobile architectures. In *Proceedings of the IEEE Conference on Computer Vision and Pattern Recognition*. 16569–16578.
- Alvaro Collet, Ming Chuang, Pat Sweeney, Don Gillett, Dennis Evseev, David Calabrese, Hugues Hoppe, Adam Kirk, and Steve Sullivan. 2015. High-quality streamable free-viewpoint video. *ACM Transactions on Graphics* 34, 4 (2015).
- Yilun Du, Yanan Zhang, Hong-Xing Yu, Joshua B. Tenenbaum, and Jiajun Wu. 2021. Neural Radiance Flow for 4D View Synthesis and Video Processing. In *Proceedings of the IEEE International Conference on Computer Vision*. 14304–14314.
- Jiemin Fang, Taoran Yi, Xinggang Wang, Lingxi Xie, Xiaopeng Zhang, Wenyu Liu, Matthias Nießner, and Qi Tian. 2022. Fast dynamic radiance fields with time-aware neural voxels. In *SIGGRAPH Asia 2022 Conference Papers*. 1–9.
- Sara Fridovich-Keil, Giacomo Meanti, Frederik Rahbæk Warburg, Benjamin Recht, and Angjoo Kanazawa. 2023. K-planes: Explicit radiance fields in space, time, and appearance. In *Proceedings of the IEEE Conference on Computer Vision and Pattern Recognition*. 12479–12488.
- Sara Fridovich-Keil, Alex Yu, Matthew Tancik, Qinhong Chen, Benjamin Recht, and Angjoo Kanazawa. 2022. Plenoxels: Radiance Fields without Neural Networks. In *Proceedings of the IEEE Conference on Computer Vision and Pattern Recognition*. 5491–5500.
- Kyle Genova, Forrester Cole, Avneesh Sud, Aaron Sarna, and Thomas Funkhouser. 2020. Local Deep Implicit Functions for 3D Shape. In *Proceedings of the IEEE/CVF Conference on Computer Vision and Pattern Recognition*. 4856–4865.
- Peter Hedman, Pratul P Srinivasan, Ben Mildenhall, Jonathan T Barron, and Paul Debevec. 2021. Baking neural radiance fields for real-time view synthesis. In *Proceedings of the IEEE International Conference on Computer Vision*. 5875–5884.
- C. Jiang, A. Sud, A. Makadia, J. Huang, M. Nießner, and T. Funkhouser. 2020. Local Implicit Grid Representations for 3D Scenes. In *Proceedings of the IEEE Conference on Computer Vision and Pattern Recognition*. IEEE Computer Society, Los Alamitos, CA, USA, 6000–6009.
- Hiroharu Kato, Yoshitaka Ushiku, and Tatsuya Harada. 2018. Neural 3D Mesh Renderer. In *Proceedings of the IEEE Conference on Computer Vision and Pattern Recognition*. 3907–3916.
- Bernhard Kerbl, Georgios Kopanas, Thomas Leimkühler, and George Drettakis. 2023. 3D Gaussian Splatting for Real-Time Radiance Field Rendering. *ACM Transactions on Graphics* 42, 4 (2023).
- Samuli Laine, Janne Hellsten, Tero Karras, Yeongho Seol, Jaakko Lehtinen, and Timo Aila. 2020. Modular primitives for high-performance differentiable rendering. *ACM Transactions on Graphics* 39, 6 (2020), 1–14.
- Lingjie Liu, Jiatao Gu, Kyaw Zaw Lin, Tat-Seng Chua, and Christian Theobalt. 2020. Neural sparse voxel fields. *Proceedings of the Advances in Neural Information Processing Systems* 33 (2020), 15651–15663.
- Stephen Lombardi, Tomas Simon, Jason Saragih, Gabriel Schwartz, Andreas Lehrmann, and Yaser Sheikh. 2019. Neural volumes: learning dynamic renderable volumes from images. *ACM Transactions on Graphics* 38, 4 (2019).
- Stephen Lombardi, Tomas Simon, Gabriel Schwartz, Michael Zollhoefer, Yaser Sheikh, and Jason Saragih. 2021. Mixture of volumetric primitives for efficient neural rendering. *ACM Transactions on Graphics* 40, 4 (2021), 1–13.
- Matthew M Loper and Michael J Black. 2014. OpenDR: An approximate differentiable renderer. In *Proceedings of the European Conference on Computer Vision*. 154–169.
- Jonathon Luiten, Georgios Kopanas, Bastian Leibe, and Deva Ramanan. 2023. Dynamic 3d gaussians: Tracking by persistent dynamic view synthesis. *arXiv preprint arXiv:2308.09713* (2023).
- Lars Mescheder, Michael Oechsle, Michael Niemeyer, Sebastian Nowozin, and Andreas Geiger. 2019. Occupancy Networks: Learning 3D Reconstruction in Function Space. In *Proceedings of the IEEE Conference on Computer Vision and Pattern Recognition*. 4455–4465.
- Ben Mildenhall, Pratul P. Srinivasan, Matthew Tancik, Jonathan T. Barron, Ravi Ramamoorthi, and Ren Ng. 2020. NeRF: Representing Scenes as Neural Radiance Fields for View Synthesis. In *Proceedings of the IEEE International Conference on Computer Vision*.
- Thomas Müller, Alex Evans, Christoph Schied, and Alexander Keller. 2022. Instant neural graphics primitives with a multiresolution hash encoding. *ACM Transactions on Graphics* 41, 4 (2022), 1–15.
- Jacob Munkberg, Jon Hasselgren, Tianchang Shen, Jun Gao, Wenzheng Chen, Alex Evans, Thomas Müller, and Sanja Fidler. 2022. Extracting Triangular 3D Models, Materials, and Lighting From Images. In *Proceedings of the IEEE Conference on Computer Vision and Pattern Recognition*. 8280–8290.
- Michael Niemeyer, Lars Mescheder, Michael Oechsle, and Andreas Geiger. 2019. Occupancy Flow: 4D Reconstruction by Learning Particle Dynamics. In *Proceedings of the IEEE International Conference on Computer Vision*. 5378–5388.
- Jeong Joon Park, Peter Florence, Julian Straub, Richard Newcombe, and Steven Lovegrove. 2019. DeepSDF: Learning Continuous Signed Distance Functions for Shape Representation. In *Proceedings of the IEEE Conference on Computer Vision and Pattern Recognition*. 165–174.
- Keunhong Park, Utkarsh Sinha, Jonathan T. Barron, Sofien Bouaziz, Dan B Goldman, Steven M. Seitz, and Ricardo Martin-Brualla. 2021a. Nerfies: Deformable Neural Radiance Fields. In *Proceedings of the IEEE International Conference on Computer Vision*. 5845–5854.
- Keunhong Park, Utkarsh Sinha, Peter Hedman, Jonathan T. Barron, Sofien Bouaziz, Dan B Goldman, Ricardo Martin-Brualla, and Steven M. Seitz. 2021b. HyperNeRF: a higher-dimensional representation for topologically varying neural radiance fields. *ACM Transactions on Graphics* 40, 6 (2021).
- Sida Peng, Junting Dong, Qianqian Wang, Shangzhan Zhang, Qing Shuai, XiaoWei Zhou, and Hujun Bao. 2021a. Animatable Neural Radiance Fields for Modeling Dynamic Human Bodies. In *Proceedings of the IEEE International Conference on Computer Vision*.
- Songyou Peng, Michael Niemeyer, Lars Mescheder, Marc Pollefeys, and Andreas Geiger. 2020. Convolutional Occupancy Networks. In *Proceedings of the European Conference on Computer Vision*. 523–540.
- Sida Peng, Yuanqing Zhang, Yinghao Xu, Qianqian Wang, Qing Shuai, Hujun Bao, and XiaoWei Zhou. 2021b. Neural body: Implicit neural representations with structured latent codes for novel view synthesis of dynamic humans. In *Proceedings of the IEEE Conference on Computer Vision and Pattern Recognition*. 9054–9063.
- Albert Pumarola, Enric Corona, Gerard Pons-Moll, and Francesc Moreno-Noguer. 2021. D-NeRF: Neural Radiance Fields for Dynamic Scenes. In *Proceedings of the IEEE Conference on Computer Vision and Pattern Recognition*. 10313–10322.
- Nikhila Ravi, Jeremy Reizenstein, David Novotny, Taylor Gordon, Wan-Yen Lo, Justin Johnson, and Georgia Gkioxari. 2020. Accelerating 3D Deep Learning with Py-Torch3D. *arXiv:2007.08501* (2020).
- Shunsuke Saito, Zeng Huang, Ryota Natsume, Shigeo Morishima, Hao Li, and Angjoo Kanazawa. 2019. Pifu: Pixel-Aligned Implicit Function for High-Resolution Clothed Human Digitization. In *Proceedings of the IEEE International Conference on Computer Vision*. 2304–2314.
- Shunsuke Saito, Tomas Simon, Jason Saragih, and Hanbyul Joo. 2020. PIFuHD: Multi-Level Pixel-Aligned Implicit Function for High-Resolution 3D Human Digitization. In *Proceedings of the IEEE Conference on Computer Vision and Pattern Recognition*. 81–90.



- Vincent Sitzmann, Justus Thies, Felix Heide, Matthias Nießner, Gordon Wetzstein, and Michael Zollhöfer. 2019. DeepVoxels: Learning Persistent 3D Feature Embeddings. In *Proceedings of the IEEE Conference on Computer Vision and Pattern Recognition*. 2432–2441.
- Liangchen Song, Anpei Chen, Zhong Li, Zhang Chen, Lele Chen, Junsong Yuan, Yi Xu, and Andreas Geiger. 2023. Nerfplayer: A streamable dynamic scene representation with decomposed neural radiance fields. *IEEE Transactions on Visualization and Computer Graphics* 29, 5 (2023), 2732–2742.
- Shih-Yang Su, Frank Yu, Michael Zollhöfer, and Helge Rhodin. 2021. A-NeRF: Articulated Neural Radiance Fields for Learning Human Shape, Appearance, and Pose. In *Proceedings of the Advances in Neural Information Processing Systems*.
- Cheng Sun, Min Sun, and Hwann-Tzong Chen. 2022. Direct voxel grid optimization: Super-fast convergence for radiance fields reconstruction. In *Proceedings of the IEEE Conference on Computer Vision and Pattern Recognition*. 5459–5469.
- Julien Valentin, Cem Keskin, Pavel Pidlypenskyi, Ameesh Makadia, Avneesh Sud, and Sofien Bouaziz. 2019. TensorFlow Graphics: Computer Graphics Meets Deep Learning.
- Liao Wang, Qiang Hu, Qihan He, Ziyu Wang, Jingyi Yu, Tinne Tuytelaars, Lan Xu, and Minye Wu. 2023. Neural Residual Radiance Fields for Streamably Free-Viewpoint Videos. In *Proceedings of the IEEE Conference on Computer Vision and Pattern Recognition*. 76–87.
- Guanjun Wu, Taoran Yi, Jiemin Fang, Lingxi Xie, Xiaopeng Zhang, Wei Wei, Wenyu Liu, Qi Tian, and Xinggang Wang. 2023. 4d gaussian splatting for real-time dynamic scene rendering. *arXiv preprint arXiv:2310.08528* (2023).
- Cheng-hsin Wu, Ningyuan Zheng, Scott Ardisson, Rohan Bali, Danielle Belko, Eric Brockmeyer, Lucas Evans, Timothy Godisart, Hyowon Ha, Alexander Hypes, et al. 2022. Multiface: A dataset for neural face rendering. *arXiv preprint arXiv:2207.11243* (2022).
- Yuxin Yao, Bailin Deng, Weiwei Xu, and Juyong Zhang. 2023. Fast and robust non-rigid registration using accelerated majorization-minimization. *IEEE Transactions on Pattern Analysis and Machine Intelligence* (2023).
- Alex Yu, Ruilong Li, Matthew Tancik, Hao Li, Ren Ng, and Angjoo Kanazawa. 2021. Plenotrees for real-time rendering of neural radiance fields. In *Proceedings of the IEEE International Conference on Computer Vision*. 5752–5761.